Bar Buckling in RC Columns Confined with Composite Materials

D. A. Bournas[1] and T. C. Triantafillou, M.ASCE[2]

Abstract: The onset and evolution of bar buckling at the plastic hinge of old-type reinforced concrete (RC) columns confined with composite material [fiber-reinforced polymer (FRP) and textile-reinforced mortar (TRM)] jackets was investigated experimentally and analytically in this study. The interaction between composite jacket (or concrete cover, for unconfined concrete) and embedded longitudinal compression reinforcement at the onset and evolution of bar buckling was achieved through strain measurements of the compression reinforcement. Moreover, the implementation of a recent stress-strain confinement model, which relates lateral with axial strains, allowed the description and monitoring of the axial-lateral strain relationship at the base of the columns throughout the evolution of bar buckling. Based on the aforementioned model and the experimental measurements, the postbuckling behavior of columns was related to the jacket stiffness. Finally, a semiempirical expression that gives the drift ratio of RC columns at the onset of bar buckling was modified herein for the case of FRP- or TRM-jacketed columns. **DOI: 10.1061/(ASCE)CC.1943-5614.0000180.**

CE Database subject headings: Bars; Buckling; Confinement; Fiber reinforced polymer; Reinforced concrete; Seismic effects; Rehabilitation; Composite materials.

Author keywords: Bar buckling; Confinement; FRP; Reinforced concrete; Seismic retrofitting; Textile-reinforced mortar (TRM).

Introduction and Background

In old-type reinforced concrete (RC) columns with inadequately detailed transverse reinforcement, where the length of the bar between successive points of restraint (successive stirrups) is significant as a multiple of the bar diameter, the longitudinal bars will possibly buckle under a critical level of compressive stress. When such columns, which have high aspect moment/shear ratios (e.g., greater than four) and adequate lap-splicing of longitudinal bars, are subjected to seismic loading, buckling of the longitudinal bars normally precipitates their ultimate failure and typically marks the limit of their usable deformation capacity. Even if bar buckling does not precipitate compressive failure of the adjacent concrete, it constitutes a key damage state which calls for extensive repairs. Additionally, it is likely that the bar that has buckled will rupture in tension immediately afterward upon reversal of the seismic excitation.

The stability of longitudinal compressive reinforcement has been investigated up to date in numerous experimental and analytical studies (Mau 1990; Monti and Nuti 1992; Gomes and Appleton 1997; Pantazopoulou 1998; Rodriguez et al. 1999; Dhakal and Maekawa 2002; Bae et al. 2005). The main parameter investigated by almost every researcher was the unsupported length of reinforcing bars in respect to their diameter, expressed by the ratio of stirrup spacing to bar diameter, s_h/d_b. This ratio in the aforementioned studies ranged between 2 and 12. On the basis of experimental and analytical results, all researchers suggested that with a proper quantity of transverse reinforcement, namely, a critical (low) value of the ratio s_h/d_b, it is possible to achieve satisfactory behavior beyond yielding of longitudinal bars in compression. This critical ratio required to prevent premature bar buckling, which was also found to depend on longitudinal bars' yield stress, varied between 6 and 8 as the yield stress of bars decreased. However, in existing old-type RC columns where the stirrup spacing is excessive (200–500 mm), the ratio s_h/d_b receives quite high values; for longitudinal bar diameters ranging from 20–12 mm, the s_h/d_b ratio varies from 10 to 42, respectively.

Monti and Nuti (1992) and Bae et al. (2005) investigated systematically the load-carrying capacity of reinforcing bars under compression, including the effect of buckling. According to their experimental results (Fig. 1), it was observed that the postbuckling behavior of reinforcing bars was quite sensitive to the s_h/d_b ratio. Especially for values of s_h/d_b greater than six, the bars evinced instability after maximum load, which was followed by a gradual drop of load-carrying capacity with increasing strains. For high values of the axial compressive strains, in the order of 0.1 to 0.15, the average postbuckling stress became practically constant after it had dropped significantly to approximately 20%–50% of the yield stress. It is worth noting here that the development of such high axial compressive strains after bar buckling could normally have been reproduced only in concentric compression tests.

The effectiveness of confinement with FRP and the newly developed textile-reinforced mortars, or TRM (Triantafillou et al. 2006), against bar buckling has been addressed to date only for the case of concentric compression. Tastani et al. (2006) investigated in a systematic way, both experimentally and analytically, the interaction between FRP jackets and embedded longitudinal compression reinforcement by testing 27 short prismatic RC columns up to failure under concentric compression. The main conclusion of this work was that the deformation capacity of FRP-jacketed members is limited by bar buckling. Similar observations

[1]Postdoctoral Researcher, European Laboratory for Structural Assessment, IPSC, JRC, T.P. 480, I-21020 Ispra (VA), Italy (corresponding author). E-mail: dionysios.bournas@jrc.ec.europa.eu

[2]Professor, Dept. of Civil Engineering, Univ. of Patras, Patras GR-26500, Greece. E-mail: ttriant@upatras.gr

Note. This manuscript was submitted on June 7, 2010; approved on October 5, 2010; published online on October 9, 2010. Discussion period open until November 1, 2011; separate discussions must be submitted for individual papers. This paper is part of the ***Journal of Composites for Construction***, Vol. 15, No. 3, June 1, 2011. ©ASCE, ISSN 1090-0268/2011/3-393–403/$25.00.

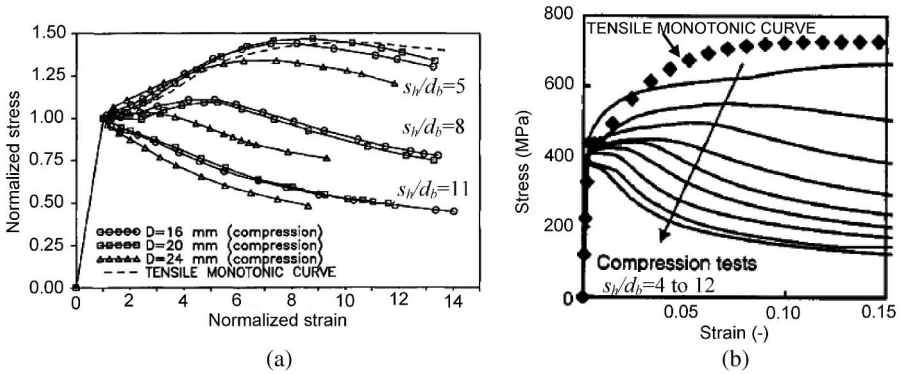

Fig. 1. Compressive stress-strain curves for reinforcing bars based on the experimental works of (a) Monti and Nuti (1992); (b) Bae et al. (2005)

have been made by Bournas et al. (2007) on the basis of the experimental results of FRP- and TRM-jacketed RC prisms, in which failure of the jackets resulted from stretching both by concrete dilation and by outward bending of the longitudinal bars in the middle of the specimens. However, contrary to pure compression conditions, the behavior and failure mechanism of FRP- and TRM-confined members is completely different when they are subjected to seismic loading.

The evolution of damage in RC columns subjected to cyclic lateral deformations is controlled by a series of complex interactions. Previous experimental research (Moyer and Kowalsky 2003; Syntzirma et al. 2010) suggests that the occurrence of bar buckling is linked to the displacement history imposed to RC columns because the latter determines the magnitude of tensile excursion that the longitudinal reinforcement undergoes prior to being stressed in compression. In addition, the effect of cycling on the constitutive properties of the concrete and steel is significant (Monti and Nuti 1992; Gomes and Appleton 1997; Rodriguez et al. 1999). Last but not least, the moment gradient along the length of the column that is subjected to reverse cyclic loading will create a strain gradient in the column's longitudinal direction.

The compressive strain of concrete is maximum at the extreme compression fiber and at the cross section of maximum moment. In this fiber, the compressive concrete receives some additional confinement from the adjacent regions of less stressed concrete, enabling the compression zone to sustain higher compressive strains. This superior behavior of columns wrapped with composite material jackets (TRM and especially FRP) applied at their plastic hinge region has been affirmed by numerous test results. However the interaction between confining jacket and embedded longitudinal compression reinforcement at the onset of bar buckling and at the postbuckling range has not been addressed to date for columns subjected to seismic loading.

In the present study, the writers investigate experimentally and analytically the evolution of bar buckling in unconfined and in FRP- or TRM-confined full-scale columns subjected to seismic loading, with a focus on understanding the effectiveness of TRM jackets. The interaction between jacket (or concrete cover for unconfined concrete) and embedded longitudinal compression reinforcement at the onset and evolution of bar buckling was achieved through strain measurements of the compression reinforcement. Thus, it was possible to address the effect of bar buckling on the response and failure mode of unconfined and TRM-confined old-type RC columns. Moreover, the postbuckling behavior of columns was related to the stiffness of the jacket.

Experimental Program

Test Specimens, Materials, and Strengthening Procedures

Four full-scale RC column specimens with the same geometry were constructed and tested under lateral load (Fig. 2). The specimens

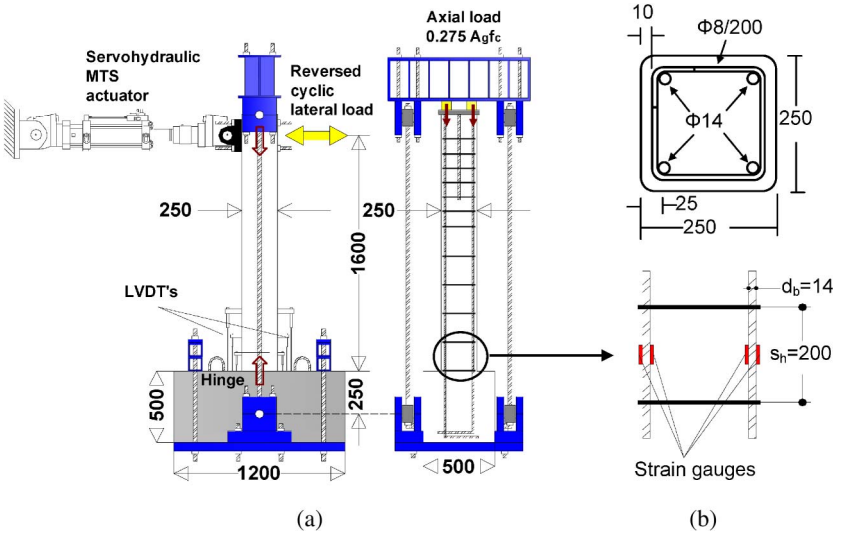

Fig. 2. (a) Schematic of test setup; (b) cross section of columns and position of strain gauges on longitudinal bars (dimensions in mm)

were flexure-dominated cantilevers with a height to the point of application of the load (shear span) of 1.6 m (half a typical story height) and a cross section of 250×250 mm. The columns were fixed into a heavily reinforced 0.5 m-deep base block, 1.2×0.5 m in plan, within which the longitudinal bars were anchored with 90° hooks at the bottom. To represent old-type nonseismically designed and detailed columns, all specimens were reinforced longitudinally with four 14-mm-diameter deformed bars with an effective depth of 225 mm and 8-mm-diameter smooth stirrups at a spacing of 200 mm, closed with 90° hooks at both ends.

One specimen was tested without retrofitting as control (L0_C), the second was retrofitted with a double-layered CFRP jacket (specimen L0_R2), the third was retrofitted with an equal (to its FRP counterpart) stiffness and strength carbon fiber TRM jacket comprising four layers (specimen L0_M4), and the last specimen was retrofitted with a lower stiffness and strength four-layered glass fiber TRM jacket (specimen L0_M4G), to investigate the effect of TRM jacket stiffness on bar buckling. Note that the layers in the carbon fiber TRM-jacketed column were twice as many compared with its FRP counterpart, resulting in the FRP and TRM jackets being of equal stiffness and strength in the circumferential direction.

The jackets extended from the base of each column (a gap of about 10 mm was left) to a height of 430 mm. The overlapping length of the jacket was equal to 150 mm. Prior to jacketing, the four corners of the columns that received jacketing were rounded at a radius equal to 25 mm.

The longitudinal bars had a yield stress of 523 MPa, a tensile strength of 624 MPa and an ultimate strain equal to 12%. The corresponding values for the steel used for stirrups were 351 MPa, 444 MPa and 19.5%, respectively. The average compressive strength on the day of testing the columns, measured on 150×150 mm cubes, was equal to 28.6 MPa.

For the specimens receiving TRM jacketing (L0_M4, L0_M4_G), two commercial textiles with equal quantity of carbon or glass rovings in two orthogonal directions were used. Each roving was 3 mm wide, and the clear spacing between rovings was 7 mm. The weights of carbon and glass fibers in the textiles were 348 g/m^2 and 480 g/m^2, respectively, and the nominal thickness of each layer (based on the equivalent smeared distribution of fibers) was 0.095 mm and 0.089 mm, respectively. The mean tensile strengths of the carbon and glass fibers (and of the textiles, when the nominal thickness is used) were taken from two datasheets and were equal to 3,800 MPa and 1,700 MPa, respectively. The elastic moduli of carbon and glass fibers were 225 GPa and 70 GPa, respectively.

For specimen L0_R2 receiving resin adhesive bonding, a commercial structural adhesive (two-part epoxy resin with a mixing ratio 3:1 by weight) with a tensile strength of 70 MPa and an elastic modulus of 3.2 GPa (cured for 7 days at 23°C) was used; those properties were provided by the manufacturer. For the specimens receiving mortar as a binding material, a commercial inorganic dry binder consisting of cement and polymers at a ratio of about 8:1 by weight was used. The water-binder ratio in the mortar was 0.23:1 by weight, resulting in plastic consistency and good workability. The strength of mortar used in this study was obtained through flexural and compression testing according to EN 1015–11 (European Committee for Standardization 1993) using a servohydraulic MTS testing machine. The average flexural and compressive strength values were 6.51 MPa and 20.8 MPa, respectively.

Experimental Setup and Procedure

To simulate seismic excitation, the columns were subjected to lateral cyclic loading, which consisted of successive cycles progressively increasing by 5 mm of displacement amplitude in each direction. At the same time, a constant axial compressive load corresponding to 27.5% of the members' compressive strength was applied to the columns. The lateral load was applied using a horizontally positioned 250-kN MTS actuator, and the axial load was exerted by a set of four hydraulic cylinders with automated pressure self-adjustment, which acted against two vertical rods connected to the strong floor of the testing frame through a hinge [Fig. 2(a)]. Displacements, rotations, and curvatures at the plastic hinge region were monitored using six rectilinear displacement transducers (three on each side, perpendicular to the piston axis) fixed at cross sections one, two and three at distances of $\ell_1 = 130$ mm, $\ell_2 = 260$ mm, and $\ell_3 = 450$ mm, respectively, from the column base, as shown in Fig. 2(a). The instrumentation also comprised a total of 8 strain gauges for each column. As shown in Fig. 2(b), two strain gauges were mounted on each reinforcing bar at a height of 100 mm from the base cross section to estimate the strain of longitudinal bars at the onset of buckling. This location was chosen because buckling is expected to occur at the midheight between the first two stirrups above the column base.

Test Results and Discussion

Detailed results in terms of load-displacement hysteresis loops, curvature, and energy dissipation are given in a previous study (Bournas et al. 2009). In this paper, the writers present only those additional test results related to the investigation of bar buckling. The response of all columns tested is given in Fig. 3 in the form of load-drift ratio envelope curves. Key results are also presented in Table 1, which include (a) the peak resistance in the two directions of loading, (b) the drift ratio corresponding to peak resistance in the two directions of loading, (c) the drift ratio corresponding to initiation of longitudinal bar buckling as the latter is defined in the next section, and (d) the drift ratio at conventional "failure" of the column, defined as reduction of peak resistance in a cycle below 80% of the maximum recorded resistance in that direction of loading. For specimen L0_M4, the reduction of peak resistance when the stroke of the horizontally positioned actuator was exhausted (at a drift ratio of 7.81%) was less than 20% of the maximum recorded resistance in both directions of loading. In this case, the drift ratio at conventional "failure" is simply stated as $> 7.81\%$.

Definition of the Onset of Bar Buckling

In most published experimental studies, one may identify considerable variation in the definition of the critical axial strain at the onset of bar buckling. This may be attributed to a number

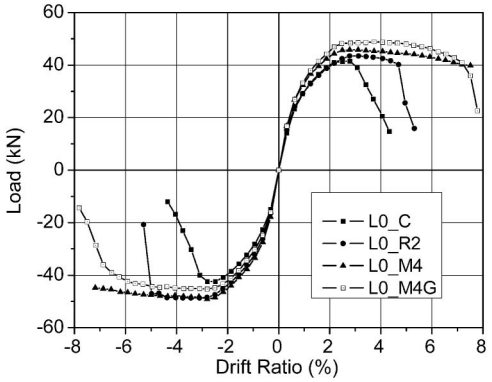

Fig. 3. Load versus drift ratio envelope curves

Table 1. Summary of Test Results

Specimen notation	Peak force (kN)		Drift at peak force (%)		Drift at initiation of bar buckling (%)		Drift at "failure" (%)	
	Push	Pull	Push	Pull	Push	Pull	Push	Pull
L0_C	41.63	−42.48	2.5	2.5	3.1	—[a]	3.43	3.43
L0_R2	43.46	−48.70	2.8	3.1	4.31	4.06	5.0	−5.31
L0_M4	45.77	−49.19	2.8	2.8	4.37	4.37	> 7.81	> 7.81
L0_M4G	48.82	−45.28	4.0	2.8	5.31	—[a]	7.5	6.9

[a]There are no reliable strain gauge recordings.

of different reasons: (a) different researchers may define the onset of buckling in different ways; (b) the experimental conditions of the various may differ; and (c) sometimes the initiation of buckling is observed with delay through oversight. To avoid this variability, in the present study the definition of the onset of bar buckling was based on direct measurements obtained by strain gauges. As mentioned previously, the positions in which the strain gauges were affixed was chosen to coincide with the locations where bar buckling was expected to occur, namely, the midheight between the first two stirrups above the column base [Figs. 2(b) and 4].

From these strain gauge measurements (Fig. 4), it is clear that bar buckling initiates in the loading cycle in which a jump in the compressive strains of longitudinal bars was recorded. Significant difference was observed between the compressive strains measured by the two strain gauges mounted in the same level and positioned around each bar. Fig. 4 illustrates the strain histories of longitudinal bars at the location where buckling was expected to occur. It is clear that for almost all specimens, buckling of longitudinal bars initiated yielding in compression and particularly in the next loading cycle. An exception is column L0_R2, in which bar buckling initiated three cycles after yielding of rebars in compression. The onset of bar buckling immediately after their yielding in compression was more or less expected, because the axial (and lateral) resistance of steel rebars at the yield plateau region is marginal (near zero stiffness).

For all columns tested in this study (externally confined or not), the compressive strain of longitudinal bars at the onset of buckling is quite close, with an average value equal to 0.70%; the measured strains vary between 0.58–0.82%, as shown in Table 2. This is because the onset of bar buckling is a kinematic phenomenon, which depends primarily on a critical value of a bar's lateral strain (outward bending of bars), after which the bar loses stability. In the case of old-type RC columns, where the buckling length is approximately equal to the stirrup spacing, this critical lateral bar compressive strain depends almost exclusively on the value of the s_h/d_b ratio. Therefore, all measured axial strains of bars at the onset of buckling were fairly close and irrespective of the confinement provided by FRP or TRM jackets. An estimation of the compressive bars' critical strain at the onset of their buckling can be made by the following expression:

$$\varepsilon_s^{cr} \approx \varepsilon_c^{cr} = 0.02(s_h/d_b)^{-0.4} \tag{1}$$

where ε_c^{cr} and ε_s^{cr} = the critical strain of concrete and longitudinal bars, respectively, at the onset of buckling of the latter. Eq. (1) has been proposed by Pantazopoulou 1998 for the estimation of concrete's critical strain at the onset of bar buckling, for $s_h/d_b > 1.5$. Considering that the strain compatibility is valid up to the initiation

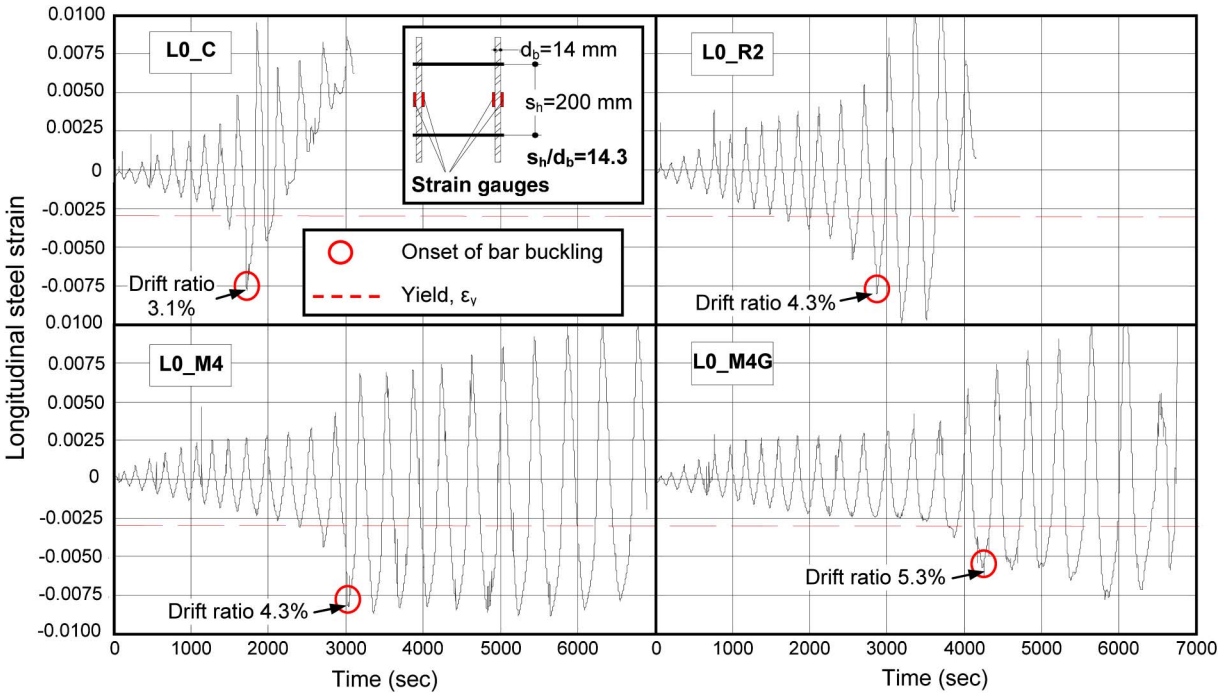

Fig. 4. Typical strain histories of longitudinal bars located at columns' base between successive stirrups

Table 2. Strains in Bars, Concrete, and Jacket at Onset of Bar Buckling and at Failure, Ratio of $\theta_{bb,\exp}/\theta_{u,\exp}$

	Compressive axial strain in longitudinal bars ε_s		Axial strain in concrete ε_c		Composite jacket strain in the circumferential direction ε_f		
Specimen notation	Onset of bar buckling	Failure	Onset of bar buckling	Failure	Onset of bar buckling	Failure	$\theta_{bb,\exp}/\theta_{u,\exp}$
L0_C	−0.0077	−0.0042	0.0063	0.0069	—	—	0.90
L0_R2	−0.0058	−0.0097	0.0064	0.0068	0.006	0.0064	0.82[a]
L0_M4	−0.0082	—	0.0093	0.0156[b]	0.0064	0.011[b]	0.56[b]
L0_M4G	−0.0063	−0.0078	0.0095	0.0109	0.0138	0.0159	0.73

[a]Controlled by failure at the unconfined length, outside the jacket.
[b]Magnitudes reached at the end of the test without conventional failure.

of bar buckling and that the values of strains in compressive steel bars and in the extreme compression fiber of concrete are approximately equal, Eq. (1) can be applied here for the determination of ε_s^{cr}. For the value of the ratio s_h/d_b corresponding to the columns tested in this study, the theoretical value of ε_s^{cr} calculated from Eq. (1) is equal to 0.69%, which is in excellent agreement with the measured strains at the onset of bar buckling. Note here that the strain plateau of the steel was in the range from 0.29% to 2.4%.

It should be pointed out here that the critical compressive strain at the onset of bar buckling, found to depend exclusively on the s_h/d_b ratio herein, may be also influenced by the thickness of the concrete cover. If the cover was much thicker, it would prevent lateral bar movement and the compressive strain at the onset of buckling would likely be different. For the specimens studied herein, the FRP and TRM jackets do not start confining significantly until the cover cracks. Because the cover was the same for all specimens, the compressive strain at buckling onset was the same. However, different cover thicknesses could likely result in different behavior, as for example delay in buckling for larger covers (which would provide higher confinement).

Control Specimen

The response of the control specimen (L0_C) was characterized by flexural yielding of the longitudinal bars, followed by their buckling and concrete cover spalling above the base. Whereas in the majority of the experimental studies it is stated that bar buckling follows concrete cover spalling or that these two phenomena are interdependent, the experimental behavior of control specimen revealed another interpretation. In the current study, the evolution of failure at the plastic hinge of specimen L0_C was maintained through the experimental observations and the measurements of strain gauges. It was observed that concrete cover spalling was caused, or at least accelerated substantially, by the onset of bar buckling. Although the concrete cover spalling was not practically measurable during the test, a careful observation at the column's base one cycle before, during, and one cycle after the onset of bar buckling is quite enlightening.

As clearly shown in Fig. 5(a), in the cycles preceding the initiation of bar buckling, namely, up to the 9th cycle, in the push direction of loading, there were not visible vertical cracks indicating concrete cover separation. In contrast, in the following 10th loading cycle in which the onset of bar buckling was recorded (drift ratio 3.1%), a few vertical cracks appeared suddenly [Fig. 5(b)], indicating the initiation of concrete cover separation. Spalling of the concrete cover was accelerated in the subsequent 11th loading cycle, as can be observed in Fig. 5(c), since the cover had been detached by the initiation of bar buckling in the previous loading cycle. In summary, based on the response of the control specimen, it can be pointed out that the onset of longitudinal bar buckling precedes concrete cover spalling and is indeed responsible for the initiation and evolution of the latter.

As determined experimentally, concrete cover spalling is attributed to the intense outward bending of bars at section's corners at the onset of bar buckling. The outward bending of bars leads to a lateral displacement w at the middle of the buckling or unsupported length $L = s_h$. This transverse displacement w has been correlated experimentally and analytically with the critical axial strain of bars during the evolution of buckling by Bae et al. (2005). By using a universal testing machine with two LVDTs, one to measure axial displacements (and axial strains) and one to monitor transverse displacements [Fig. 6(a)], Bae et al. (2005) managed to monitor simultaneously both axial and transverse displacements. Their experimental results [Fig. 6(b)] show that the relationship of transverse displacement w and axial critical strain ε_s of a buckled bar can be expressed as a bilinear line, with slope depending on the s_h/d_b ratio. The following equation was proposed for this purpose (Bae et al. 2005):

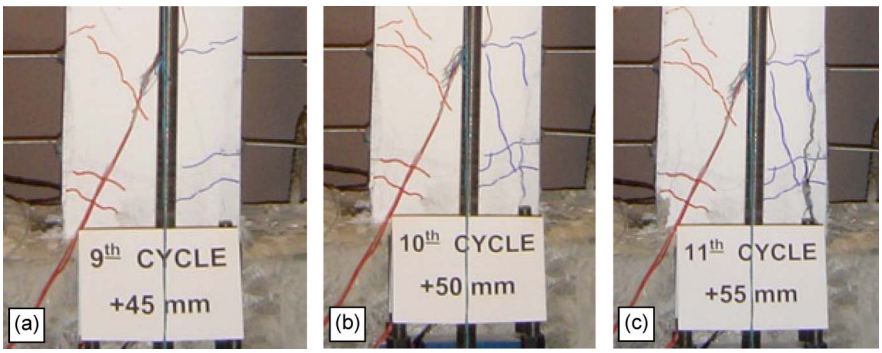

Fig. 5. Evolution of concrete cover separation and spalling owing to bar buckling at the base of the column L0_C: (a) one cycle before; (b) during; and (c) one cycle after the initiation of bar buckling

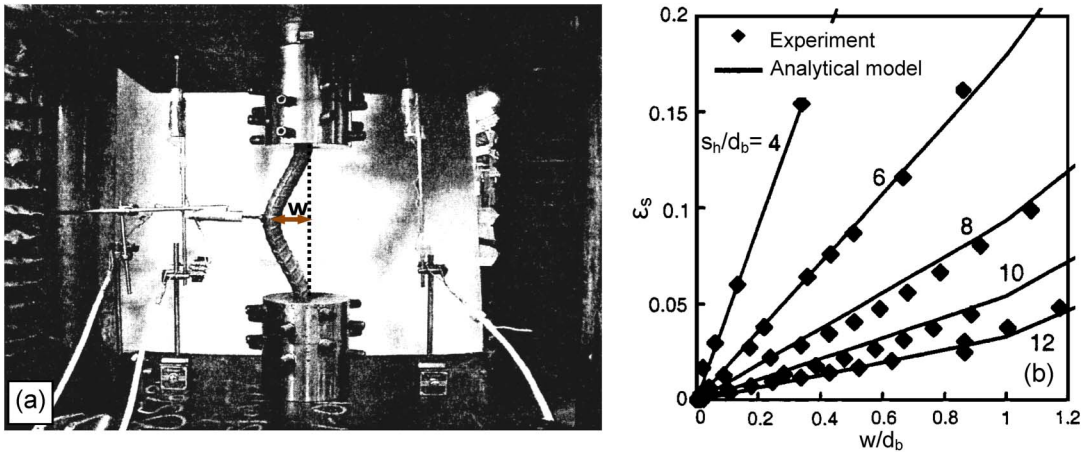

Fig. 6. (a) Test setup; (b) experimental results about axial strain–transverse displacement predictions of Bae et al. (2005)

$$\varepsilon_s = \max\left\{\left(\frac{0.035\cos\theta+\theta}{\cos\theta-0.035\theta}\right)\frac{w}{d_b}, \left(\frac{0.07\cos\theta+\theta}{\cos\theta-0.07\theta}\right) \times \left(\frac{w}{d_b}-0.035\right)\right\} \quad (2)$$

where

$$\theta = \frac{6.9}{(s_h/d_b)^2} - 0.05 \quad (3)$$

Application of Eqs. (2) and (3) for the values of the ratio s_h/d_b and the experimentally measured critical axial strain ε_s^{cr} of the control specimen results in a lateral deflection w equal to 5.74 mm. Thus, this approximately calculated transverse deflection at the onset of (symmetric) buckling at the midheight between successive stirrups confirms what was experimentally observed, namely, that bar buckling is responsible for spalling of the concrete cover.

Effectiveness of TRM and FRP Jackets against Bar Buckling

The behavior and failure mode of confined columns (L0_R2, L0_M4, and L0_M4G) was not controlled by longitudinal bar buckling above the column base. According to measurements of strain gauges (Fig. 4) placed on longitudinal bars inside the jackets, even though a significant delay ranging from three to seven cycles with respect to their unretrofitted counterpart (L0_C) was observed, without lateral strength degradation, bar buckling was not averted for FRP- or TRM-confined specimens. This is attributed to the behavior of buckled bars under external confinement. These bars could sustain a significant part of their compressive load after buckling because the concrete cover spalled, remained in place, and provided lateral support.

For FRP- or TRM-confined columns subjected to cyclic bending under axial load, the critical point that determines whether failure will or will not occur during the evolution of bar buckling is the available excess compressive strength of confined concrete; the latter should override the unsustainable part of the buckled bars' compressive stress. If failure at that point of load redistribution from buckled bars to the surrounding confined concrete is suppressed, the effectiveness of FRP or TRM confinement is not limited by premature bar buckling. Thus, jacket confinement extends substantially the deformation capacity of the column.

Consider, for example, the two TRM-jacketed specimens L0_M4 and L0_M4G tested in the present study. Because bar buckling was controlled inside the TRM jackets, the axial strains of longitudinal bars remained almost constant after the onset of bar buckling (Fig. 4). Thus, the compressive bars did not lose a high percentage of their compressive load-carrying capacity. More specifically, based on the axial stress-strain curves of Fig. 1 and on the compressive strains measured on bars, it could be calculated that the residual compressive capacity of buckled bars is in the order of 50–90% of their yield stress. Additionally, by considering that the height of the compression zone is in the range between 20–60% of the height h of the columns' section, one could determine the demand in strength increase for TRM-confined concrete in order to prevent column failure during bar buckling. This is applied herein for the more conservative case in which the residual compressive strength of buckled bars is equal to 50% of their yield stress. It is finally derived that the strength increase for the TRM-confined concrete core should be only 2.1 MPa and 6.4 MPa, respectively, for the cases of the narrower and deeper compression zones. It is therefore clear that these minimal increases in compressive strength are easily provided by the confinement.

Although cross-sectional analysis indicates that bar buckling does not seem to be critical for columns confined with composite jackets, it may not be eliminated entirely. Especially for columns confined with FRP jackets, two different failure modes are possible:

- Abrupt bar buckling above the FRP jacket. The confinement provided by the FRP jacket to Specimen L0_R2 restrained the outward bending of longitudinal bars inside the FRP jacket region. Owing to this fact, the concrete cover dilation was marginal, and a large amount of strain energy was stored in the confined concrete without any stress relaxation in the compression zone. This resulted in the transition of the compressive force above the FRP jacket, where buckling of longitudinal bars finally occurred abruptly in the space between the FRP jacket's end and the next stirrup. Similar observations of bar buckling above the FRP jacket in regions with significantly lower bending moment than that of the column base have been made by other researchers (e.g., Bousias et al. 2007).
- Bar buckling often occurs at the detriment of the jacket owing to premature failure by rupture of fibers. The primary reason for that is the poor resistance of FRPs against localized stress concentrations that necessarily develop around the midpoint between successive stirrups in poorly detailed members when

Fig. 7. Lateral expansion of TRM jackets at the base of RC columns without fiber rupture

the principal compression reinforcement becomes unstable (Tastani and Pantazopoulou 2004).

Contrary to specimen L0_R2, rebar buckling in columns L0_M4 and L0_M4G developed gradually inside the TRM-jacketed area, as the compressive force released from early buckled bars was carried by the surrounded confined concrete inside the jackets. This can occur in a confining system because TRM jackets are able to deform outward without early fiber rupture, owing to the relatively low composite action between fibers and mortar that allows for higher local deformations (e.g., slip of fibers within rovings), as shown in Fig. 7. Thus, if longitudinal bars bend outward at the corners of the section during buckling, TRM jackets receive the developed stress concentrations without failure. Note here that the TRM jackets demonstrated similar performance against bar buckling of near-surface mounted (NSM) steel bars (Bournas and Triantafillou 2009). Additionally, in the present study, TRM jackets allowed the buckled bars to deform slightly outward at the corners, enabling relaxation of compression stresses, which in turn prevented the transition of abrupt bar buckling above the jacket.

Lateral-Axial Strain Relationship for TRM- and FRP-Confined Members

Concrete confined with FRP or TRM jackets, contrary to steel transverse reinforcement that applies a constant confining pressure after yielding, experiences an increasing level of confining pressure with increasing lateral strain. The level of confining pressure is proportional to the concrete's lateral dilation, which in turn is a function of the stiffness of the confining material. Because of this interaction, the relation between axial and lateral strains is derived implicitly in most of the models of FRP-confined concrete (e.g. Mirmiran and Shahawy 1996; Spoelstra and Monti 1999; Fam and Rizkalla 2001; Chun and Park 2002; Harries and Kharel 2002; Marques et al. 2004); hence, an iterative procedure is necessary to generate the stress-strain curves. Because of this complexity, it is inconvenient for such models to be directly used in design.

On the basis of a careful interpretation of test results of unconfined, actively confined, and FRP-confined specimens, Teng et al. (2007) developed a new stress-strain model for FRP-confined concrete, in which the response of the concrete core and the FRP jacket, as well as their interaction, were considered explicitly. According to this model, the axial-lateral strain relationship is

$$\frac{\varepsilon_c}{\varepsilon_{co}} = 0.85\left(1 + 8\frac{\sigma_l}{f'_{co}}\right)\left\{\left[1 + 0.75\left(\frac{-\varepsilon_l}{\varepsilon_{co}}\right)\right]^{0.7} - \exp\left[-7\left(\frac{-\varepsilon_l}{\varepsilon_{co}}\right)\right]\right\} \quad (4)$$

where ε_c = axial strain of concrete and ε_{co} = strain at peak f_c of the concrete stress-strain diagram [equal to 0.0022, based on concentric compression tests of FRP and TRM-confined prisms (Bournas et al. 2007)]. The confining pressure σ_l supplied by the jacket (FRP or TRM) for a rectangular section may be estimated as (Triantafillou et al. 2006)

$$\sigma_l = a_f \frac{(b+h)}{bh} t_f E_f \varepsilon_f \quad (5)$$

b = width of compression zone; h = cross-section side parallel to the loading direction; E_f and $\varepsilon_f = -\varepsilon_l$ = elastic modulus and strain, respectively, of the jacket in the lateral direction; t_f = thickness of one fiber sheet or textile layer; and α_f = effectiveness coefficient for confinement with fibers (FRP or TRM jackets), equal to

$$a_f = \beta\left[1 - \frac{(b-2R)^2 + (h-2R)^2}{3bh}\right] \quad (6)$$

where R = radius at corners of the cross section. The coefficient β in Eq. (6) accounts for the different effectiveness of TRM compared to FRP jackets in terms of ultimate strain. On the basis of concentric compression tests on reinforced concrete prisms presented in Bournas et al. (2007), this value is about 0.9. But if jacket failure has not been reached at conventional failure of the column, no modification should be made and β should be taken equal to 1.

Based on the average axial strain of concrete monitored at the plastic hinge region using displacement transducers [Fig. 2(a)], the corresponding lateral strains (or jacket strains) can be evaluated from Eqs. (4) and (6). In that way, the average strain of the jacket in the circumferential direction, corresponding to bar buckling $\varepsilon_f^{\text{buckl}}$ and to conventional failure $\varepsilon_f^{\text{ult}}$, can be approximately calculated for each column.

Fig. 8 presents the most important experimental and analytical results as a function of columns' drift ratio. In addition to the horizontal load, the average (in the two directions of loading) values of the following response characteristics are plotted in the figure: (a) the axial strain of the compressive bars; (b) the axial strain of concrete at the plastic hinge region (compression zone); and

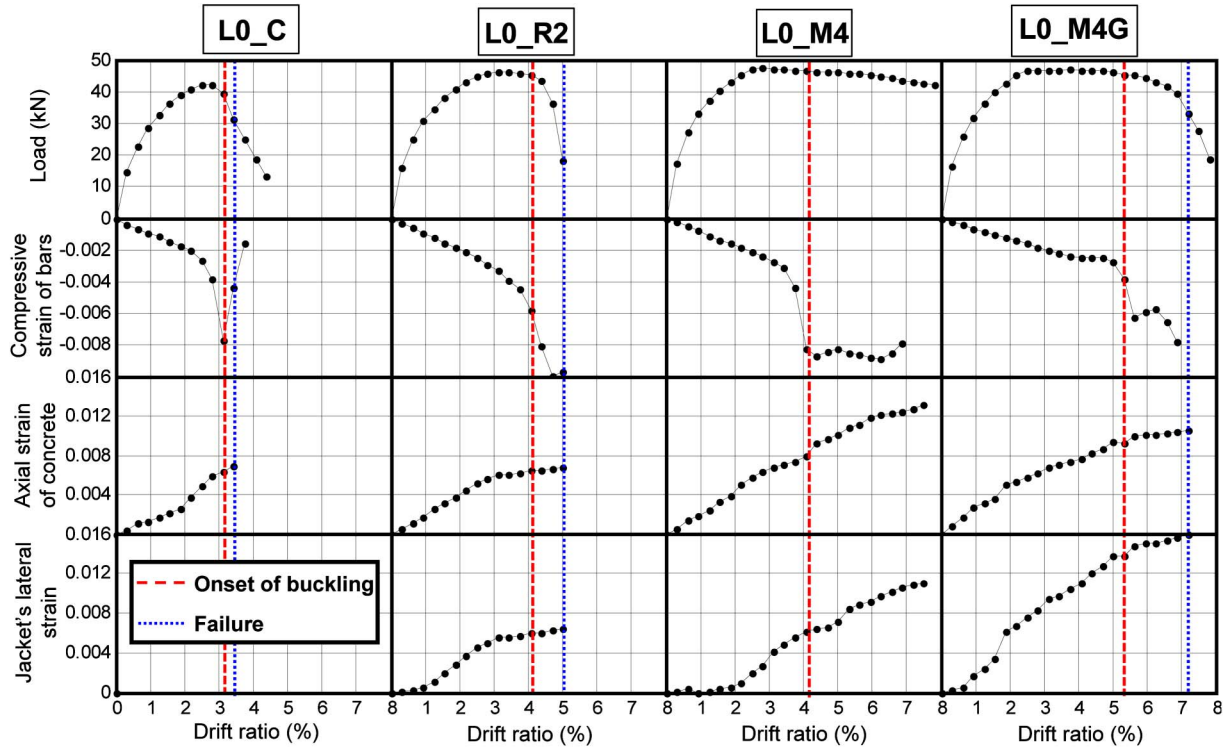

Fig. 8. Diagrams of experimental results (lateral load, axial strain of compressive bars, axial strain of concrete at the plastic hinge region, jacket strain in the lateral direction) as a function of the drift ratio

(c) the transverse strain of FRP or TRM jackets. Also, Table 2 presents the values of the above magnitudes at the onset of bar buckling and at columns' conventional failure.

For the unretrofitted specimen, it is clear that lateral strength degradation starts with the onset of bar buckling. Indeed, conventional failure takes place in the next loading cycle. It is also very clear that the postbuckling behavior of TRM-confined columns (L0_M4, L0_M4G) depends on the jacket's stiffness. Although bar buckling was controlled for both TRM-jacketed specimens, only the stiffer carbon fiber jacket (L0_M4) managed to develop high axial strains without failure.

More specifically, for the same level of concrete axial strains in the order of 1%, which was marked at the onset of bar buckling, the corresponding average transverse strains of carbon and glass fiber TRM jackets were equal to 0.64% and 1.38%, respectively. Further increase of the axial strain owing to the evolution of bar buckling and expansion of concrete resulted in fracture of the glass fiber jacket and failure of the specimen L0_M4G when the average transverse strain of the jacket was equal to 1.6%. This demonstrates that the effectiveness of a relatively low stiffness composite jacket is low when high axial deformations (higher that 1%) are developed in the compression zone of RC columns. In contrast, the effectiveness of stiffer jackets is higher. The latter is confirmed by the response of column L0_M4: despite the fact that the axial strain was quite high, equal to 1.56%, at the end of test, the average transverse strain developed at the carbon fiber jacket remained at lower levels (1.1%). It should be noted here that no comparison can be made with results for specimen L0_R2 because its deformation capacity was controlled by buckling at the unconfined length above the FRP jacket.

The last column of Table 2 gives the ratio of the experimental value of the drift ratio (average value between the two directions of loading) at the onset of bar buckling, $\theta_{bb,\exp}$, over its corresponding value at conventional failure of the columns $\theta_{u,\exp}$. This ratio

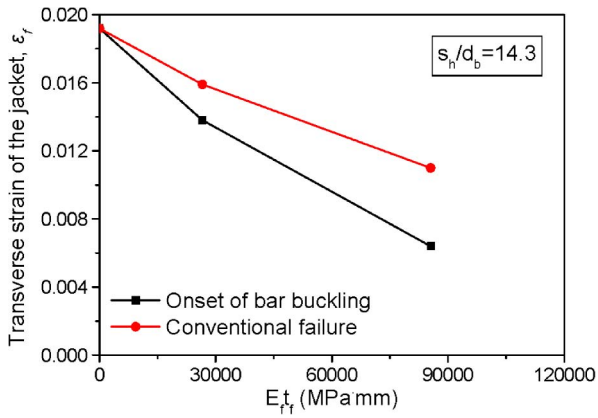

Fig. 9. TRM jacket lateral strain versus stiffness at the base of RC columns

indicates the strong dependence of the available deformation capacity of unconfined columns to bar buckling. For columns confined with TRM jackets, this dependence weakens, and a significant deformation capacity reserve is recorded from the initiation of bar buckling up to ultimate failure of these columns; this reserve increases with the increase of the TRM jacket's stiffness.

Fig. 9 presents the variation of the composite jacket's strain ε_f in the circumferential direction as a function of its stiffness at the onset of bar buckling and at conventional failure. The transverse strain for the point which corresponds to zero stiffness has been calculated through Eq. (4) for zero confining pressure ($\sigma_l = 0$) and the axial strain of the unconfined column at the onset of buckling. The main trend illustrated in Fig. 9 is that stresses in the jacket after bar buckling decrease (hence the associated margin of safety related to jacket rupture increases) almost linearly with the increase in jacket stiffness. This trend explains why the $\theta_{bb,\exp}/\theta_{u,\exp}$ ratio

decreases with stiffness. Fig. 9 should certainly be used with care because it is based on limited test results and on a specific value of the s_h/d_b ratio. More tests on FRP- or TRM-confined columns with various jacket stiffness and s_h/d_b ratios are necessary in order to provide the best fit to the above diagrams.

Determination of Drift at the Onset of Buckling

The cyclic deformation capacity of RC columns, a key property in displacement-based design used in seismic rehabilitation applications, is typically expressed through the members' attained drift ratio at failure. This important parameter for FRP- or TRM-confined columns can be predicted according to Bournas et al. (2009). However, to implement performance-based earthquake engineering, it is necessary to relate deformation demands placed on structural components with the probability of reaching specific levels of damage preceding failure. The onset of buckling of longitudinal bars in RC columns constitutes a key damage state because it requires extensive repairs but also significantly reduces the structure's functionality.

Based on the results of plastic-hinge analysis and of moment-curvature analysis, and by considering the expected influence of confinement reinforcement, Berry and Eberhard (2005) derived relationships that link the drift ratio of RC columns with the onset of bar buckling. These relationships, which account for the effective confinement ratio, axial-load ratio, moment/shear ratio and longitudinal bar diameter, were calibrated using observations of bar buckling from cyclic tests of 62 rectangular and 42 spiral-reinforced concrete columns. For practical implementation, the following relationship was proposed to approximate the drift ratio at the onset of bar buckling in reinforced concrete columns:

$$\theta_{bb\_\mathrm{calc}}(\%) = 3.25\left(1 + k_{ee\_bb}c\frac{d_b}{h}\right)(1-\nu)\left(1+\frac{L_V}{10h}\right) \quad (7)$$

where $k_{ee\_bb} = 40$ and 150 for rectangular and spiral-reinforced columns, respectively; $c = \alpha\rho_{sx}f_{yw}/f_c$; $\rho_{sx} = A_{sw}/bs_h$ = transverse steel ratio parallel to the direction x of loading; f_{yw} = yield stress of stirrups; f_c = compressive strength of concrete (MPa); a = effectiveness coefficient for confinement with stirrups; $\nu = N/bhf_c$ = normalized axial force (compression taken as positive); and $L_V = M/V$ = ratio of moment to shear at the end section.

If a column is retrofitted with an FRP or TRM jacket in the plastic hinge region, it is logical to adopt the expression in Eq. (7) with c given by the sum of two terms: one to account for the contribution of stirrups and a second to account for the contribution of the jacket, as follows:

$$c = a\rho_{sx}\frac{f_{yw}}{f_c} + a_f\rho_{fx}\frac{f_{fe}}{f_c} \quad (8)$$

where $\rho_{fx} = 2nt_f/b$; n = number of layers of the fiber sheet or textile; f_{fe} = effective strength of jacket; and α_f as defined in Eq. (6).

For the geometric and material properties of the columns tested in this study, the predicted and experimentally measured drift ratios at the onset of bar buckling are presented and compared in Table 3 for all retrofitted and unretrofitted columns. The predicted drift ratios at the onset of bar buckling according to the previously described approach based on Berry and Eberhard (2005) are 31%, 48%, and 47% higher than the experimental values of the unretrofitted (L0_C) and retrofitted columns (L0_R2 and L0_M4), respectively. For specimen L0_M4G, the predicted drift ratio at the onset of buckling is quite close to the experimental one. Note also that the comparison of the predicted to experimental drift ratio at the onset of bar buckling may be meaningless for specimen L0_R2 because its deformation capacity was controlled by the unconfined length above the FRP jacket.

Table 3. Comparison of Predictions Based on Berry and Eberhard (2005) and Experimentally Measured Drift Ratios at the Onset of Bar Buckling

Specimen notation	Experimental drift ratio at the onset of bar buckling $\theta_{bb,\mathrm{exp}}$	Prediction of drift ratio by Berry and Eberhard (2005) $\theta_{bb,\mathrm{pred}}$	$\theta_{bb,\mathrm{pred}}/\theta_{bb,\mathrm{exp}}$
L0_C	3.1	4.08	1.31
L0_R2	4.21	6.23[a]	1.48[a]
L0_M4	4.37	6.42	1.47
L0_M4G	5.31	4.98	0.93

[a]Controlled by failure at the unconfined length, outside the jacket.

It can be concluded that the formulation based on Berry and Eberhard (2005), as modified here for columns with continuous deformed bars jacketed with FRP or TRM, overestimates the drift ratio at the onset of bar buckling. This is likely because in the present study the initiation of bar buckling was monitored directly through strain gauges. On the contrary, in the experiments included in the database of Berry and Eberhard (2005) there is not such a provision in recording the onset of bar buckling, which is observed with delay in subsequent loading cycles.

Conclusions

In the present study, the evolution of bar buckling was investigated experimentally and analytically in unconfined and FRP- or TRM-confined large-scale columns subjected to seismic loading. The effectiveness of confinement with composite jackets and the interaction between jacket or concrete cover (for unconfined concrete) and embedded longitudinal compression reinforcement at the onset and evolution of bar buckling were addressed. A careful interpretation of the experimental and analytical results leads to more specific conclusions, which are summarized in a rather qualitative manner as follows:

- The critical axial strain ε_s^{cr} at the onset of bar buckling depends on the value of the s_h/d_b ratio. All measured axial strains of bars at the onset of buckling had, irrespective of the confinement provided by FRP or TRM jackets, fairly close values, with an average value equal to 0.70%. This is because the onset of bar buckling is a kinematic phenomenon that depends primarily on a critical value of the bar's lateral strain (outward bending), after which the bar loses stability.
- Bar buckling initiated for almost all columns immediately after their yielding in compression owing to the nearly zero axial resistance (axial stiffness) of steel rebars at the yield plateau region.
- It seems that in the case of old-type RC columns (specimen L0_C), the concrete cover separation above the base is attributed to bar buckling. Thus, spalling of the concrete cover, which leads to a drop in the horizontal load resistance, is accelerated by bar buckling.
- Bar buckling was not averted for FRP- or TRM-confined specimens; it developed with a significant delay, ranging from three to seven cycles, with respect to their unretrofitted counterpart (L0_C). Even when it initiated, bar buckling was controlled and was not accompanied by lateral strength degradation. It seems that through FRP or TRM confinement it is possible to achieve redistribution of the compressive overload to the core

from the bars as the latter reach conditions of instability. This is attributed to the behavior of buckled bars under external confinement, which could sustain a significant part of their compressive load after buckling because the concrete cover spalling remained in place and provided lateral support.

- TRM jackets allow for higher local deformations because, contrary to FRP jackets, they are able to deform outward without early fiber rupture. Thus, during buckling, when longitudinal bars bend outward at the corners of the section, TRM jackets receive the developed stress concentrations without failure.
- When high axial strains (in the order of 1%) developed in the compression zone of the columns, the lower stiffness glass fiber TRM jacket bulged and ruptured. On the other hand, the effectiveness of the stiffer carbon fiber TRM jacket on column L0_M4 was higher; while the axial strain at the end of the test was quite high (1.56%), the average transverse strain remained far from its tensile capacity.
- A substantial deformation capacity reserve from the onset of bar buckling up to the columns' conventional failure was recorded. This reserve increases with the increase of the TRM jacket's stiffness.
- The semiempirical formulation of Berry and Eberhard (2005), as modified here for columns confined with composite materials (FRP or TRM jackets), overestimates the drift ratio at the onset of bar buckling.

Acknowledgments

The writers wish to thank Assistant Professor C. Papanicolaou for her assistance in the experimental program. The work reported in this paper was funded by the Greek General Secretariat for Research and Technology through the project ARISTION, within the framework of the program "Built Environment and Management of Seismic Risk."

Notation

The following symbols are used in this paper:

A_{sw} = area of transverse steel reinforcement parallel to direction x within s_h;
b = cross-section width, width of compression zone;
d_b = diameter of longitudinal bars;
E_f = elastic modulus of jacket in the lateral direction;
f_c = compressive strength of concrete;
f_{co} = compressive strength of unconfined concrete;
f_{fe} = effective stress of jacket at conventional failure of column;
f_{yw} = yield stress of stirrups;
h = cross-section height, side parallel to the loading direction;
k_{ee_bb} = coefficient;
L_V = ratio of moment to shear at end section;
ℓ_i = distance of cross section i from column base, $i = 1, 2, 3$;
M = moment at end section;
N = axial force;
n = number of layers;
R = radius at corners of rectangular cross section;
s_h = spacing of stirrups;
t_f = thickness of one fiber sheet or textile layer;
V = shear at end section;
w = lateral displacement at middle of buckling or unsupported length $L = s_h$;
α = effectiveness coefficient for confinement with stirrups;
α_f = effectiveness coefficient for confinement with fibers;
β = TRM versus FRP jacket confining effectiveness in terms of strength;
ε_c = axial strain of concrete;
ε_{co} = strain at peak of concrete stress-strain diagram;
$\varepsilon_f^{\text{buckl}}$ = jacket's average transverse strain at onset of bar buckling;
$\varepsilon_f^{\text{ult}}$ = jacket's average transverse strain owing to concrete dilation at failure;
ε_c^{cr} = critical axial strain of concrete at onset of bar buckling;
$\varepsilon_f = -\varepsilon_\ell$ = jacket strain in the lateral direction;
ε_s = axial strain of longitudinal reinforcement;
ε_s^{cr} = critical axial strain of longitudinal reinforcement at onset of buckling;
$\theta_{bb,\text{calc}}$ = predicted drift ratio at onset of bar buckling;
$\theta_{bb,\text{exp}}$ = experimental drift ratio at onset of bar buckling;
$\theta_{u,\text{exp}}$ = drift ratio at ultimate;
ν = normalized axial force;
ν_u = Poisson ratio at failure;
ρ_{fx} = ratio of fibers parallel to direction x of loading;
ρ_{sx} = transverse steel ratio parallel to direction x of loading; and
σ_ℓ = lateral stress owing to jacketing.

References

Bae, S., Mieses, A. M., and Bayrak, O. (2005). "Inelastic buckling of reinforcing bars." *J. Struct. Eng.*, 131(2), 314–321.

Berry, M. P., and Eberhard, M. O. (2005). "Practical performance model for bar buckling." *J. Struct. Eng.*, 131(7), 1060–1070.

Bournas, D. A., Lontou, P. V., Papanicolaou, C. G., and Triantafillou, T. C. (2007). "Textile-reinforced mortar (TRM) versus FRP confinement in reinforced concrete columns." *ACI Struct. J.*, 104(6), 740–748.

Bournas, D. A., and Triantafillou, T. C. (2009). "Flexural strengthening of RC columns with NSM FRP or stainless steel." *ACI Struct. J.*, 106(4), 495–505.

Bournas, D. A., Triantafillou, T. C., Zygouris, K., and Stavropoulos, F. (2009). "Textile-reinforced mortar (TRM) versus FRP jacketing in seismic retrofitting of RC columns with continuous or lap-spliced deformed bars." *J. Compos. Constr.*, 13(5), 360–371.

Bousias, S. N., Spathis, A.-L., and Fardis, M. N. (2007). "Seismic retrofitting of columns with lap spliced smooth bars through FRP or concrete jackets." *J. Earthquake Eng.*, 11(5), 653–674.

Chun, S. S., and Park, H. C. (2002). "Load carrying capacity and ductility of RC columns confined by carbon fiber reinforced polymer." *Proc., 3rd Int. Conf. on Composites in Infrastructure* (CD-ROM), Univ. of Arizona, San Francisco.

Dhakal, P. R., and Maekawa, K. (2002). "Modelling for postyield buckling of reinforcement." *J. Struct. Eng.*, 128(9), 1139–1147.

European Committee for Standardization. (1993). "Methods of test for mortar for masonry—Part 11: Determination of flexural and compressive strength of hardened mortar." *EN 1015–11*, Brussels.

Fam, A. Z., and Rizkalla, S. H. (2001). "Confinement model for axially loaded concrete confined by circular fiber-reinforced polymer tubes." *ACI Struct. J.*, 98(4), 451–461.

Gomes, A., and Appleton, J. (1997). "Nonlinear cyclic stress-strain relationship of reinforcing bars including buckling." *Eng. Struct.*, 19(10), 822–826.

Harries, K. A., and Kharel, G. (2002). "Behavior and modeling of concrete subject to variable confining pressure." *ACI Mater. J.*, 99(2), 180–189.

Marques, S. P. C., Marques, D. C. S. C., da Silva, J. L., and Cavalcante, M. A. A. (2004). "Model for analysis of short columns of concrete confined

by fiber-reinforced polymer." *J. Compos. Constr.*, 8(4), 332–400.
Mau, S. (1990). "Effect of tie spacing on inelastic buckling of reinforcing bars." *ACI Struct. J.*, 87(6), 671–677.
Mirmiran, A., and Shahawy (1996). "A new concrete-filled hollow FRP composite column." *Composites, Part B*, 27(3–4), 263–268.
Monti, G., and Nuti, C. (1992). "Nonlinear cyclic behaviour of reinforcing bars including buckling." *J. Struct. Eng.*, 118(12), 3268–3284.
Moyer, M. J., and Kowalsky, G. (2003). "Influence of tension strain on buckling of reinforcement in concrete columns." *ACI Struct. J.*, 100(1), 78–85.
Pantazopoulou, S. J. (1998). "Detailing for reinforcement stability in RC members." *J. Struct. Eng.*, 124(6), 623–632.
Rodriguez, M. E., Botero, J. C., and Villa, J. (1999). "Cyclic stress-strain behaviour of reinforcing steel including effect of buckling." *J. Struct. Eng.*, 125(6), 605–612.
Spoelstra, M. R., and Monti, G. (1999). "FRP-confined concrete model." *J. Compos. Constr.*, 3(3), 143–150.
Syntzirma, D. V., Pantazopoulou, S. J., and Aschheim, M. (2010). "Load-history effects on deformation capacity of flexural members limited by bar buckling." *J. Struct. Eng.*, 136(1), 1–11.
Tastani, S. P., and Pantazopoulou, S. J. (2004). "Experimental evaluation of FRP jackets in upgrading RC corroded columns with substandard detailing." *Engineering Structures*, 26(6), 817–829.
Tastani, S. P., Pantazopoulou, S. J., Zdoumba, D., Plakantaras, V., and Akritidis, E. (2006). "Limitations of FRP jacketing in confining old-type reinforced concrete members in axial compression." *J. Compos. Constr.*, 10(1), 13–25.
Teng, J. G., Huang, Y. L., Lam, L., and Ye, L. P. (2007). "Theoretical model for fiber-reinforced polymer-confined concrete." *J. Compos. Constr.*, 11(2), 201–210.
Triantafillou, T. C., Papanicolaou, C. G., Zissimopoulos, P., and Laourdekis, T. (2006). "Concrete confinement with textile-reinforced mortar jackets." *ACI Struct. J.*, 103(1), 28–37.